JOURNAL OF GEOPHYSICAL RESEARCH, VOL. 112, D24S22, doi:10.1029/2007JD008956, 2007

Click Here for Full Article

Spatial and temporal characteristics of the decadal abrupt changes of global atmosphere-ocean system in the 1970s

Dong Xiao[1,2] and Jianping Li[3]

Received 2 May 2007; revised 18 September 2007; accepted 19 October 2007; published 11 December 2007.

[1] Using NOAA extended reconstruction SST (ERSST.v2) and NCEP/NCAR reanalysis, a moving *t* test technique is employed to detect the decadal abrupt change years (DACYs) in the time series of several atmosphere-ocean variables. The decadal abrupt changes (DACs) existed widely in the ocean-atmosphere system in 1973–1978. In the ocean, the decreased DACs (DDACs, the variable decreases after the DACY) occurred in the North and South Pacific and the increased DACs (IDACs, the variable increases after the DACY) mainly took place in the eastern Pacific, southern South Pacific and South Indian Ocean. In the atmosphere, the IDACs happened over the Eastern Hemispheric tropics and subtropics in the low troposphere and over the global tropics and subtropics in the middle and upper troposphere and stratosphere. The higher pressure levels, the larger the DAC regions and the later the DACYs generally. The initial oceanic DACs in the 1970s cannot be explained by the DACs of wind stress, which happened 2 years (a) later than the original oceanic DACs. In addition, the tropical influence through atmosphere and ocean cannot explain the initial DDACs of SST and atmosphere of the North Pacific, which occurred about 2 a in advance of tropical warming. The DDACs in the 1970s of the North Pacific cannot interpret that of other oceanic regions, because they were not the initial oceanic DACs in the 1970s. These findings suggest that the DACs in the 1970s may initially originate from the ocean and a coupled atmosphere-ocean decadal interaction mechanism existed in the winter of the North Pacific.

Citation: Xiao, D., and J. Li (2007), Spatial and temporal characteristics of the decadal abrupt changes of global atmosphere-ocean system in the 1970s, *J. Geophys. Res.*, *112*, D24S22, doi:10.1029/2007JD008956.

1. Introduction

[2] Recent studies present evidence that the North Pacific atmosphere-ocean system fluctuates with decadal periods [e.g., *Nitta and Yamada*, 1989; *Trenberth*, 1990; *Chen et al.*, 1992; *Graham*, 1994; *Trenberth and Hurrell*, 1994; *Graham et al.*, 1994; *Deser and Blackmon*, 1995; *Kachi and Nitta*, 1997; *Zhang et al.*, 1997; *Minobe*, 1997; *Mantua et al.*, 1997; *Nakamura et al.*, 1997; *Chao et al.*, 2000; *Wu and Liu*, 2003]. Among many manifestations of the decadal variability, the decadal abrupt changes (DACs) around 1976 were the most striking. The oceanic characteristics of the DACs were that the winter sea surface temperature (SST) in the central North Pacific dropped distinctly and the opposite trend was in the tropical Pacific and along the west coast of North America [*Nitta and Yamada*, 1989; *Zhang et al.*, 1997]. The atmospheric characteristics of the DACs in the 1970s have been explored in terms changes of deeper Aleutian low than normal, southward shift in the Pacific storm tracks [*Trenberth and Hurrell*, 1994], weaker winter blocking activity than before [*Nakamura et al.*, 1997], more occurrences of cold-air outbreaks in winter in the eastern United States [*Dowton and Miller*, 1993], less wintertime precipitation over the northwestern Pacific and North America [*Chen et al.*, 1996; *Mantua et al.*, 1997], and warmer winters along the west coast of North America and Alaska than before [*Trenberth and Hurrell*, 1994]. The DACs around 1976 also influenced the epipelagic ecosystems in the North Pacific [*Mantua et al.*, 1997; *Chavez et al.*, 2003]. These studies mainly focus on the winter characteristics of the decadal variability over the North Pacific. The characteristics of the DACs in the 1970s of other seasons and their diversities are less focused.

[3] While not conclusive in terms of the causes and mechanisms of the decadal variability over the North Pacific, several studies suggest that the decadal variability over the North Pacific is attributed to the tropical Pacific forcing [e.g., *Nitta and Yamada*, 1989; *Chen et al.*, 1992; *Graham*, 1994; *Trenberth and Hurrell*, 1994; *Graham et al.*, 1994; *Gu and Philander*, 1997; *Barnett et al.*, 1999; *Vimont et al.*, 2001]. Besides the tropical Pacific SST, the DACs over the North Pacific are also associated with that of the annual and winter SST in the tropical Indian Ocean [*Nitta and Yamada*, 1989; *Zhang et al.*, 1997; *Deser et al.*, 2004]. It is interesting whether there are any other oceanic regions

[1]College of Atmospheric Science, Lanzhou University, Lanzhou, China.
[2]Also at National Key Laboratory of Numerical Modeling for Atmospheric Sciences and Geophysical Fluid Dynamics, Institute of Atmospheric Physics, Chinese Academy of Science, Beijing, China.
[3]National Key Laboratory of Numerical Modeling for Atmospheric Sciences and Geophysical Fluid Dynamics, Institute of Atmospheric Physics, Chinese Academy of Science, Beijing, China.

Copyright 2007 by the American Geophysical Union.
0148-0227/07/2007JD008956$09.00

accompanied with these known DACs. Moreover, the DACs of subarctic front occurred 2 years (a) in advance of the tropical SST warming [*Nakamura et al.*, 1997]. We explore the temporal variations of the DACs in different regions.

[4] Several studies illustrated that the tropical SST warming influenced the frequency, intensity and onset phase of ENSO [*Trenberth and Hurrell*, 1994; *Wang*, 1995]. However, the impacts of the tropical SST warming in the 1970s on global and higher-level atmosphere are less emphasized. Borne in mind that the occurrence time of DACs may be discrepant at different atmospheric levels, we are aim to give a picture of spatial and temporal structures of the atmospheric DACs by revisiting the characteristics of the global DACs of atmosphere-ocean system in the 1970s from seasonal and multilevel views.

[5] In this study, applying moving *t* test technique (MTT) to several climate variables, including SST, upward longwave radiation flux (ULWRF), surface air temperature (SAT), sea level pressure (SLP), and 850-hPa, 500-hPa, 200-hPa, and 50-hPa geopotential heights, the horizontal characteristics of the DACs in the 1970s are documented by overlapping the temporal cross sections of the decadal abrupt change years (DACYs) from 1973 to 1978. In order to show the vertical characteristics of the atmospheric DACs, a suite of selected regions of geopotential height are detected by MTT. According to DAC extents, several time series with area weighted are examined by the MTT to show the DACs of mean value and to identify the validity of the MTT. The characteristics of the DACs of wind stress are displayed to reveal the oceanic responses to the atmosphere. All of the analyses are for boreal seasons, including annual average, spring (March–May, MAM), summer (June–August, JJA), autumn (September–November, SON), and winter (December–February, DJF).

[6] This paper is organized as follows. The method and data are outlined in next section. In section 3, the horizontal, vertical and temporal characteristics of the DACs of global atmosphere-ocean system in the 1970s are documented. In section 4, we try to explore the possible temporal relationships between the DACs of SST and the atmospheric ones. Summary and conclusion are in the last section.

2. Method and Data

2.1. Moving *t* Test Technique

[7] *Jiang and You* [1996] indicated that MTT could detect the abrupt change years (ACYs) in a time series more than once, with a certain timescale. The MTT is used to detect abrupt change through examining whether the difference between the mean values of two subsamples is significant or not. For a time series of the length n $\{X_i, i = 1, 2, \ldots, n\}$, a certain sample is selected, by moving, as a cutting point to obtain the two subsets ($\mathbf{x}_1$ and $\mathbf{x}_2$) before and after it.

[8] The *t* statistic is defined as:

$$t = \frac{\bar{x}_2 - \bar{x}_1}{s\cdot\sqrt{\frac{1}{n_1}+\frac{1}{n_2}}},$$

where $s = \sqrt{\frac{n_1 s_1^2 + n_2 s_2^2}{n_1 + n_2 - 2}}$, n_1, n_2 are the subsample sizes, namely, the detecting scales of MTT, $\bar{x}_1$, $\bar{x}_2$ are the mean values, and s_1^2, s_2^2 are the variances for the two subsets, respectively. Given a significant level α, the ACYs, namely, abrupt change points are named corresponding to the wave crests or troughs of the periods ($|t| \geq t_\alpha$).

[9] The presupposition of MTT is that the time series follows the normal distribution and the samples are independent of each other. The atmospheric and oceanic time series, which are not always following normal distribution, are preprocessed being normalized into cube root. Moreover, the DACYs are weighted by the normal distribution of both subseries of *t* test warranted by the skewness and kurtosis test (sktest) [*Huang*, 2000] as follows:

$$g_s = \frac{m_3}{m_2^{3/2}}, \quad g_k = \frac{m_4}{m_2^2} - 3, \quad m_k = \frac{1}{n}\sum_{i=1}^{n}(x_i - \bar{x})^k;$$

$$s_{g_s} = \sqrt{\frac{6(n-2)}{(n+1)(n+3)}}, \quad s_{g_k} = \sqrt{\frac{24\ n(n-2)(n-3)}{(n+1)^2(n+3)(n+5)}};$$

$$u_s = \frac{|g_s|}{s_{g_s}}, \quad u_k = \frac{|g_k|}{s_{g_k}}$$

if $u_s < 1.96$ and $u_k < 1.96$, the normal distribution hypothesis is accepted at 0.05 significant level, vice versa.

[10] In modern statistics, the degrees of freedom of *t* test of the independent and normal time series are generally adopted as:

$$f(n) = n_1 + n_2 - 2$$

The samples of the atmospheric and oceanic time series are generally not independent each other. The degrees of freedom estimated by the above formula are generally more than the effective ones. The effective degrees of freedom of *t* test are expediently evaluated by the autocorrelation coefficient of the time series [*Jiang et al.*, 2001] as:

$$E_f(n) = f(n)\left[\sum_{\tau=0}^{K} r^2(\tau)\right]^{-1}$$

where, $r(\tau)$ is the autocorrelation coefficient with a lagged scale τ; the maximum of the integer K corresponds to the value of $r^2(\tau)$ when it is close to 0.

[11] This paper focuses on decadal abrupt changes of mean value (DACMV, hereafter referred as DAC for simplicity). We take the detecting scales $n_1 = n_2 = 10$, a decadal timescale. The head and the tail of the time series are expanded 10 a with the beginning value and the ending value, respectively, so that we could capture all the DACYs in the data period. Presumed that there are *m* DACYs in a time series, the time series is divided into $m + 1$ periods. The persistence time of each period lasts equal or more than the minimum of the detecting scales, maybe except the marginal ones. Each DACY in the time series is significant by *t* test with the new detecting scales, which are the persistence time of the periods before and after the DACY.

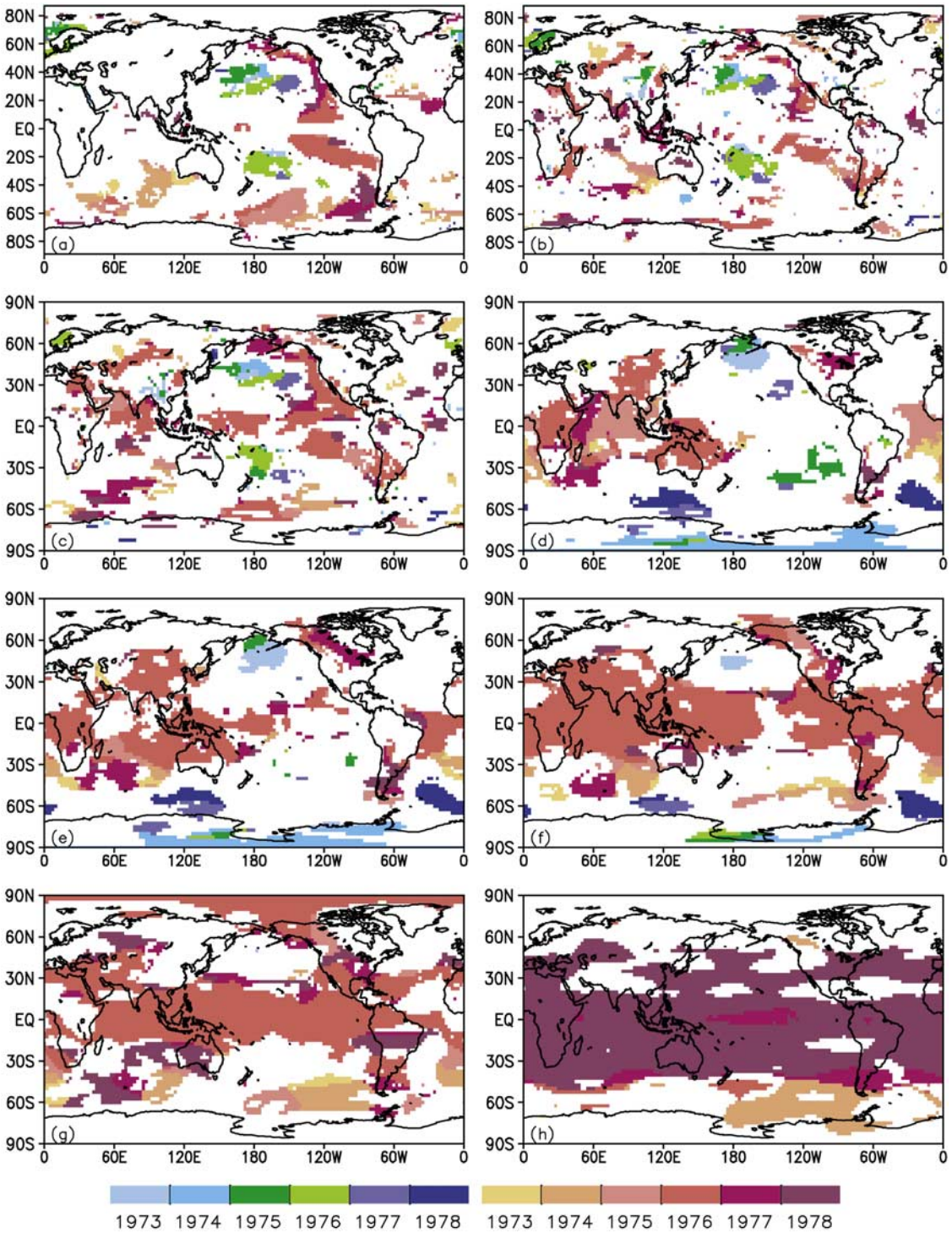

Figure 1. Horizontal distributions of the DACYs in the 1970s of annual averaged field of (a) SST, (b) ULWRF, (c) SAT, (d) SLP, and (e) 850-hPa, (f) 500-hPa, (g) 200-hPa and (h) 50-hPa geopotential heights. The cold color system (green, blue, etc.) and warm color system (yellow, red, etc.) represent the decreased DACYs and increased DACYs significant at 0.05 level, respectively. The false discovery rate of the DACYs in each field is controlled at 0.05.

[12] We employ MTT to detect the DACs in each time series in a field of atmosphere-ocean system. The horizontal and vertical distributions of the DACs of atmosphere-ocean system exist multiple testing problems that some DACs in a field might be false positive. Therefore the *Benjamini and Hochberg* [1995] multiple testing correction is adapted in this study to control the false discovery rate of the DACs in each field at 0.05.

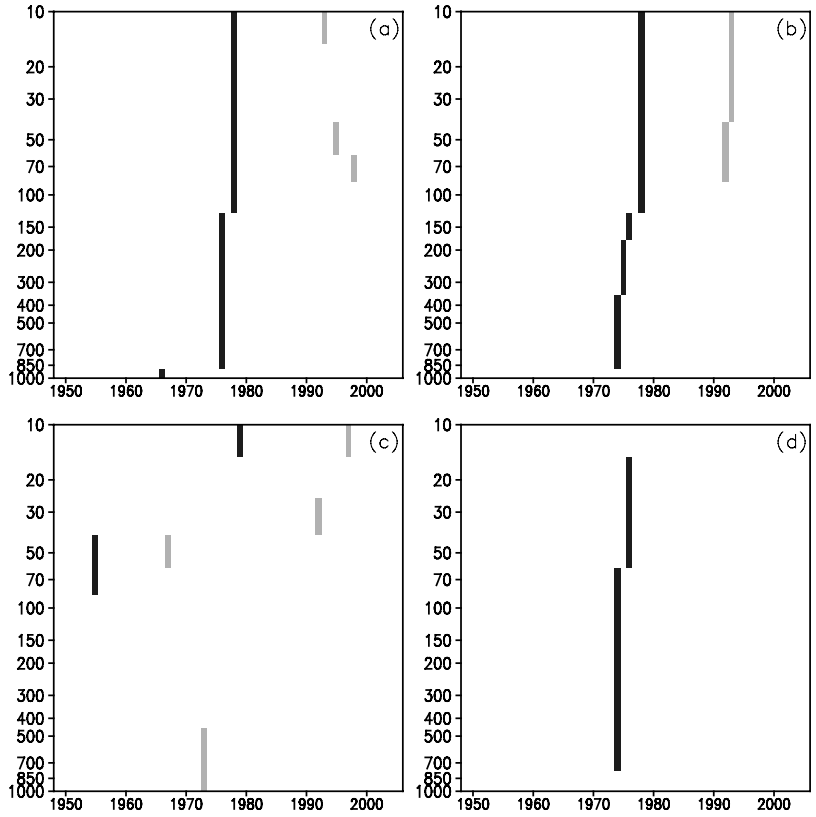

Figure 2. Vertical distributions of the DACYs of annual averaged geopotential height field in the domains (a) (30°S–30°N, 0°–357.5°E), (b) (20°–40°S, 20°W–15°E), (c) (40°–60°N, 170°E–150°W) and (d) (35°–55°S, 80°–110°E). The darker and lighter shading indicates the increased DACYs and decreased DACYs, respectively, which exceed the 0.05 significant level. The false discovery rate of the DACYs in each field is controlled at 0.05.

2.2. Data Used

[13] Monthly mean SLP, SAT and geopotential height fields in this study are obtained from the National Centers for Environmental Prediction/National Center for Atmosphere Research (NCEP/NCAR) reanalysis data sets (January 1948 to February 2007) [*Kalnay et al.*, 1996]. The data are at a 2.5° latitude × 2.5° longitude grid. The monthly mean ULWRF, got form NCEP/NCAR reanalysis data sets, is at a Gaussian grid (192 × 94). The monthly mean extended reconstruction SST (ERSST.v2) (January 1948 to February 2007) [*Smith and Reynolds*, 2004] and wind stress (January 1948 to February 2006), both based on Comprehensive Ocean-Atmosphere Data Set (COADS), are gotten from NOAA CDC. Both resolutions are 2.0° × 2.0°.

3. Horizontal, Vertical, and Temporal Characteristics of the DACs of Atmosphere-Ocean System in the 1970s

[14] The horizontal distributions of the DACYs mean the occurrence times of the DACs of different regions. The vertical distributions of the DACYs refer to the occurrence times of the DACs of different levels of certain selected regions. The DAC episode (DACE), which is not the experience time of the transition of averaged state of a time series, is a period within the minimum of the detecting scales of MTT (a decade in this study) from the beginning to the ending of the DACs event (such as the DACs in the 1970s). Each DAC increases/decreases abruptly after the DACY. The DACE of the atmosphere-ocean system in the 1970s is from 1973 to 1978. We only discuss the DACs in the 1970s and focus on larger DAC regions in this paper. We do not depict the DACs round 2000, which need be confirmed in longer data.

3.1. Annual Averaged Fields

[15] The horizontal characteristics of the DACs of several annual averaged variables are documented in Figure 1, including SST, ULWRF, SAT, SLP, and 850-hPa, 500-hPa, 200-hPa, and 50-hPa geopotential heights. In SST field, the decreased DACs (DDACs, the variable decreases after the DACY) took place in the central North Pacific in 1973–1977, in the South Pacific in 1976, and in the Norway Sea in 1974–1976. The increased DACs (IDACs, the variable increases after the DACY) happened in the southern South Pacific in 1974–1978, in the tropical eastern Pacific in 1975–1976, along the coast of North American in 1976–1978, and in the South Indian Ocean in 1973–1975. The distribution of the DACs of ULWRF (Figure 1b) and SAT (Figure 1c) is analogous to that in Figure 1a, except the DACs of the tropical Indian Ocean in 1978 and 1976, respectively. The IDACs of SLP (Figure 1d) and 850-hPa

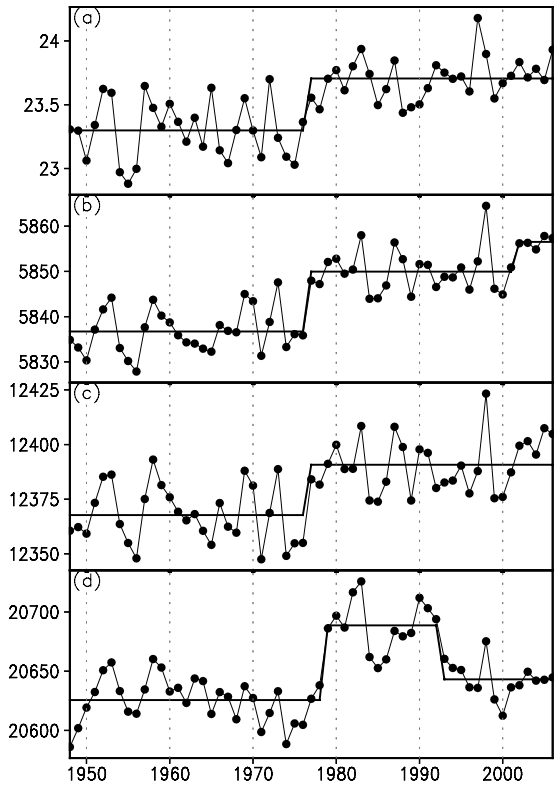

Figure 3. Annual averaged time series and episode average divided by the DACYs based on SST in the area (a) (10°–30°S, 150°–70°W) and geopotential height in the regions (b) (30°S–30°N, 0°–357.5°E) at 500 hPa, (c) (30°S–30°N, 0°–357.5°E) at 200 hPa and (d) (50°S–50°N, 0°–357.5°E) at 50 hPa. Unit is °C in Figure 3a and gpm in Figures 3b–3d. The DACYs detected by MTT all exceed the 0.01 significant level.

geopotential height (Figure 1e) took place generally over the tropics in Eastern Hemisphere in 1975–1977. The DDACs of SLP, 850-hPa and 500-hPa geopotential height (Figure 1f) occurred over the North Pacific in 1973–1975, and over the Southern Hemisphere (SH) midlatitude and high latitude in 1974, 1977–1978. The IDACs of 500-hPa (Figure 1f) and 200-hPa geopotential height (Figure 1g) happened over the South Indian Ocean in 74–1978, over the southeast Pacific in 1973–1978, over the South Atlantic in 1973–1975 and over the tropics in 1976. Figure 1h shows that the IDACs of 50-hPa geopotential height occurred over southern South Pacific in 1974 and over the tropics and subtropics in 1978.

[16] In order to disclose the vertical characteristics of geopotential height of several selected regions, Figure 2a depicts that the DACs of tropical geopotential height took place at 1000–150 hPa in 1976 and at 100–10 hPa in 1978. In a whole, the tropospheric DACs are earlier than the stratospheric ones in the 1970s. The DACs over the domain (20°–40°S, 20°W–15°E) (Figure 2b) happened at 925–400 hPa in 1974, at 300–150 hPa in 1975–1976, and at 100–10 hPa in 1978. The DDACs over the North Pacific (Figure 2c) happened at 1000–500 hPa in 1973. Figure 2d exhibits that the IDACs of the region (35°–55°S, 80°–110°E) occurred at 700–70 hPa in 1974 and at 50–20 hPa in 1976.

[17] To see the DACs of mean value more clearly, the IDACs of the southern tropical eastern Pacific SST (Figure 3a) occurred in 1976, with an enhancement 0.4°C of mean value. The tropical time series (Figures 3b, 3c and 3d) of 500-hPa, 200-hPa 50-hPa geopotential height documented the IDACs in 1976, 1976 and 1978, respectively. The mean values of the latter episode are 13.2, 23 and 63 geopotential meter (gpm) larger than the former ones, respectively.

3.2. Spring Averaged Fields

[18] The distributions of the spring averaged DACs are exhibited in Figure 4. The distribution of the DACs of SST (Figure 4a), ULWRF (Figure 4b) and SAT (Figure 4c) are similar to that of the annual averaged ones, except the DDACs of SST over the North Pacific and the DDACs of SAT along North America in 1976–1977. The IDACs of SLP (Figure 4d) and 850-hPa geopotential height (Figure 4e) took place over the tropics in the Eastern Hemisphere in 1976–1977. The IDACs of 500-hPa (Figure 4f) and 200-hPa geopotential height (Figure 4g) happened over the South Indian Ocean in 1973–1978, over the subtropical South Atlantic in 1975, and over the tropic in 1976–1977. The IDACs of 50-hPa geopotential height (Figure 4h) took place over the Drake Passage in 1973, over the southeastern Pacific in 1974, over the South Atlantic in 1976, over the tropics in 1977, and over the subtropics in 1978.

[19] Figure 5a indicates that the IDACs of the region (15°S–15°N, 0°–357.5°E) occurred at 925–300 hPa in 1976, at 250–150 hPa and 20–10 hPa in 1977, and at 100–70 hPa in 1978. The IDACs of the area (40°–50°S, 25°–50°E) over the South Indian Ocean (Figure 5b) occurred at 700–200 hPa in 1973, at 150–100 hPa in 1977, and at 70–30 hPa in 1978. The DACs of the region (20°–40°S, 25°W–5°E) (Figure 5c) took place at 850–150 hPa in 1975, at 100–70 hPa in 1978, at 50–30 hPa in 1977, and at 20–10 hPa in 1978. The DACs over the extent (50°–60°S, 75°–40°W) (Figure 5d) happened at 700–50 hPa in 1973, and at 30–10 hPa in 1977. Figure 5e describes that the IDACs of the region (25°–50°S, 80°–110°E) occurred at 850–200 hPa in 1974 and at 150–10 hPa in 1976–1978. The IDAC over the domain (35°–50°S, 160°E–165°W) (Figure 5f) happened at 1000–150 hPa in 1973, at 100 hPa in 1974, and at 70–20 hPa in 1977. Moreover, The DDACs of above regions happened in stratosphere in early 1990s.

[20] The IDACs of the southern tropical eastern Pacific SST (Figure 6a) happened in 1976, with an enhancement 0.4°C of mean value. The DACYs of the time series of tropical 850-hPa, 500-hPa and 50-hPa geopotential height (Figures 6b, 6c and 6d) lie in 1976, 1976 and 1977 and the averages of the latter states are 14.6, 26.8 and 43.9 gpm higher than the former ones, respectively.

3.3. Summer Averaged Fields

[21] Figure 7a indicates that the DACs of SST resemble that of Figure 1a, except the IDACs of the southern tropical eastern Pacific SST and the DDACs of the South Pacific SST in 1975–1976. The characteristics of the DACs of ULWRF (Figure 7b) and SAT (Figure 7c) are similar to that

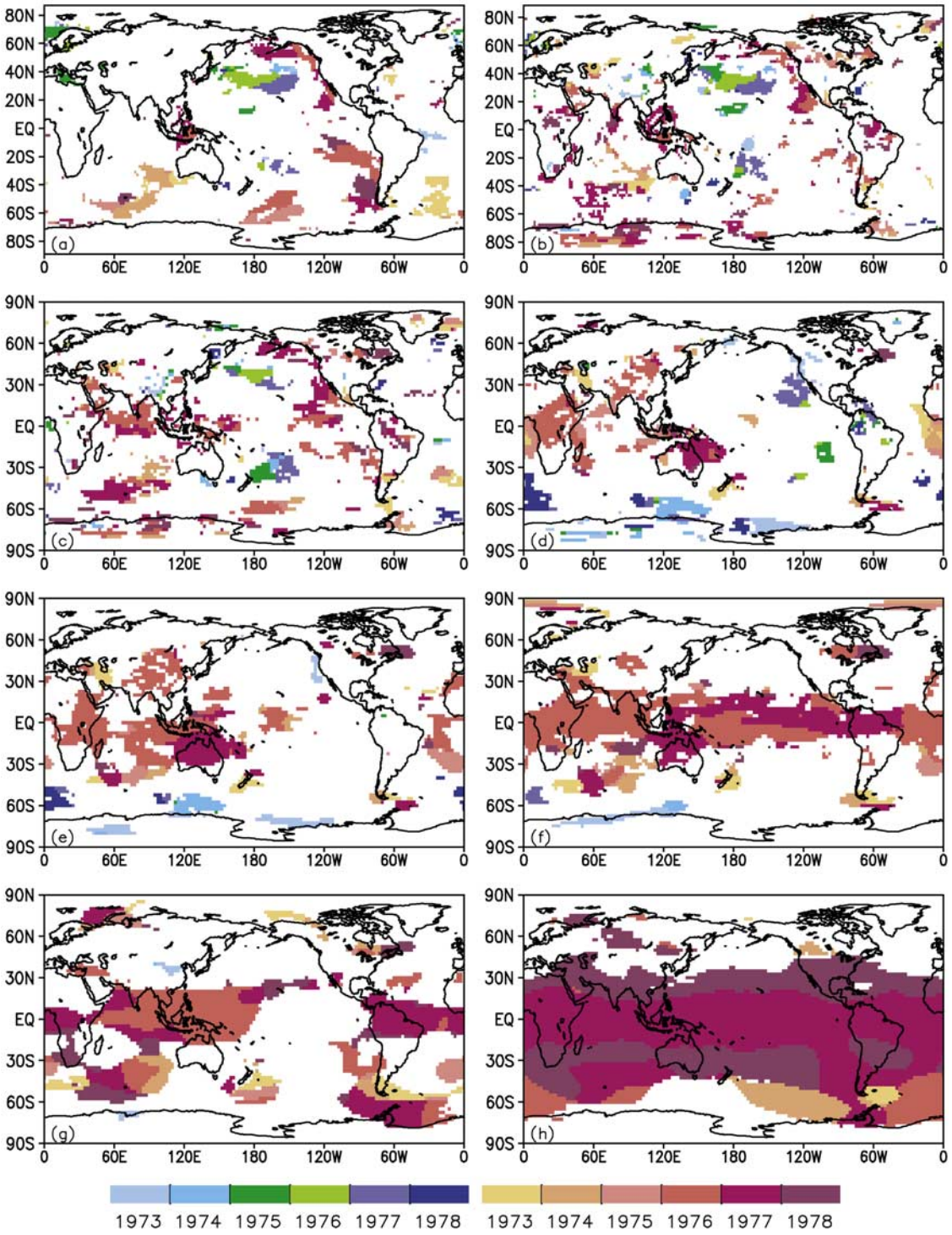

Figure 4. Same as Figure 1 but in spring averaged field.

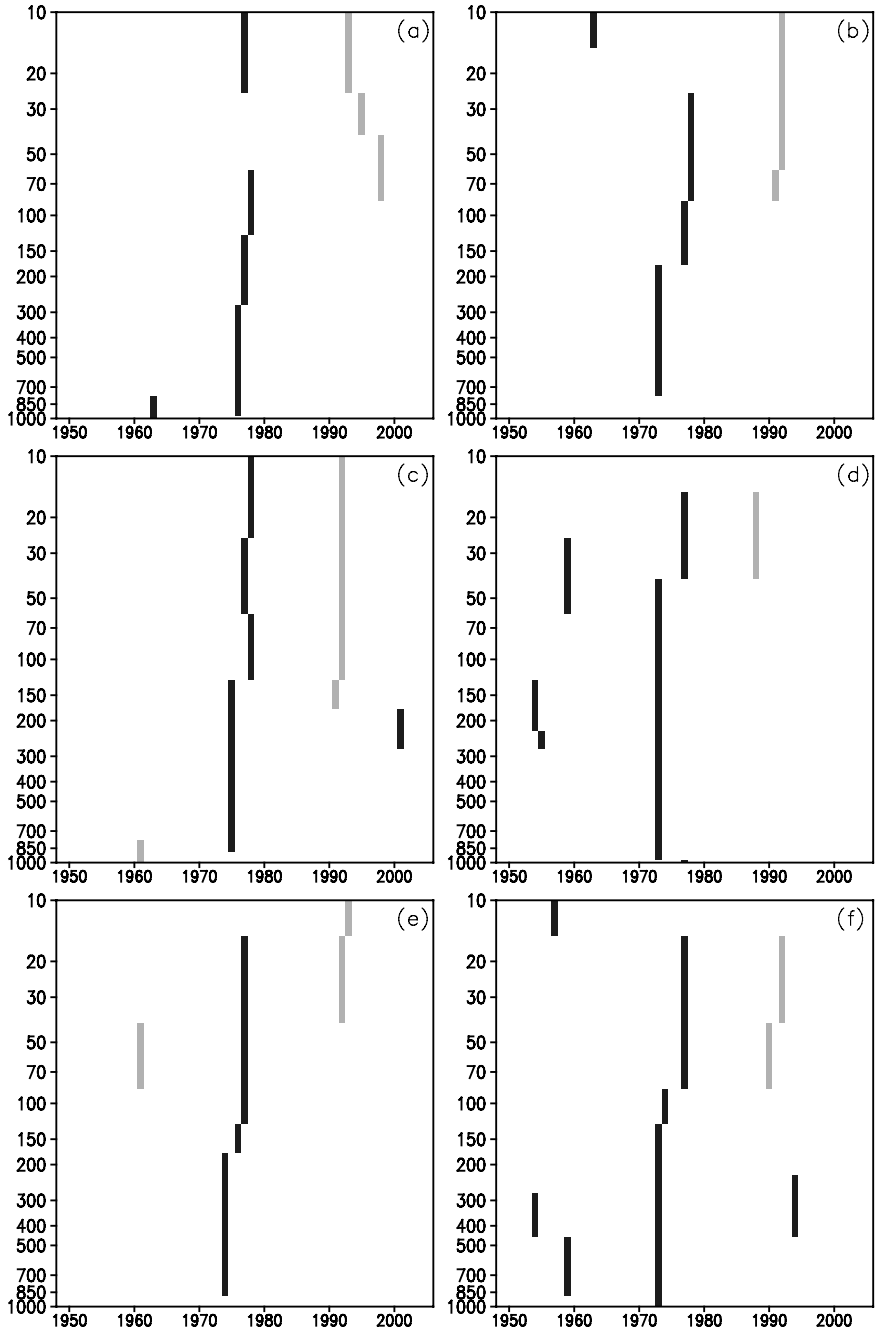

Figure 5. As in Figure 2 but in spring averaged field in the areas (a) (15°S–15°N, 0°–357.5°E), (b) (40°–50°S, 25°–50°E), (c) (20°–40°S, 25°W–5°E), (d) (50°–60°S, 75°–40°W), (e) (25°–50°S, 80°–110°E) and (f) (35°–50°S, 160°E–165°W).

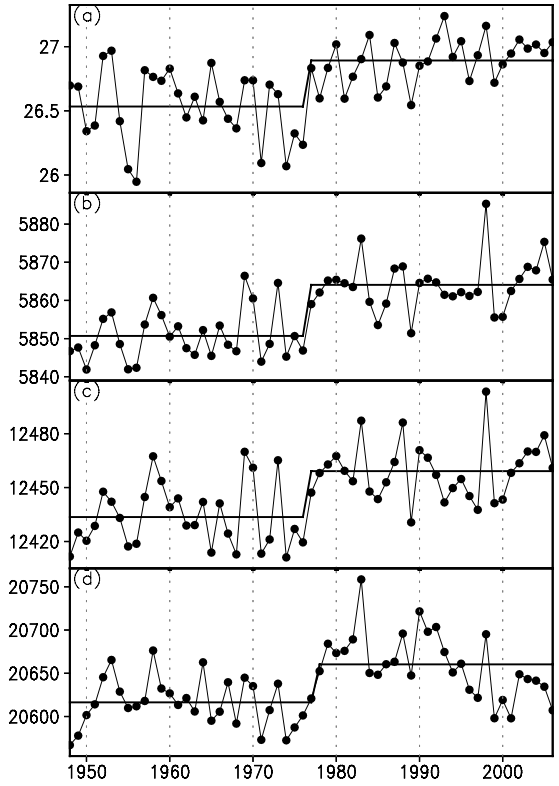

Figure 6. As in Figure 3 but in spring averaged field in the domains (a) (10–24°S, 120°–70°W), (b) (20°S–20°N, 0°–357.5°E), (c) (15°S–20°N, 60°E–180°) and (d) (20°S–20°N, 0°–357.5°E).

in Figure 7a. The IDAC of SLP (Figure 7d) and 850-hPa geopotential height (Figure 7e) happened generally over the tropics in 1975 and 1978. The characteristics of the DACs of 850-hPa geopotential height (Figure 7e) are similar to that in Figure 7d. The IDACs of 500-hPa geopotential height (Figure 7f) presented over the tropics in 1976 and 1978. The DDACs of SLP, 850-hPa and 500-hPa geopotential height took place over the Antarctica and circumpolar areas in 1974–1978. The IDACs of 200-hPa (Figure 7g) and 50-hPa geopotential height (Figure 7h) appeared over the tropics in 1978.

[22] Figure 8a shows the IDACs of tropical geopotential height presented at 1000–30 hPa in 1978, at 20–10 hPa in 1979 and at 1000–600 hPa in 1964. The IDACs in 1964 are consistent with the findings of *Li et al.* [2005]. The IDACs (Figure 9b) of the South Atlantic happened at 1000–150 hPa in 1974–1975 and at 100–20 hPa in 1978. The IDACs (Figure 8c) of the South Indian Ocean occurred at 500–50 hPa in 1974.

[23] The IDACs of the southern tropical eastern Pacific SST (Figure 9a) occurred in 1975, with an enhancement 0.58°C of mean value. Three time series of 500-hPa, 200-hPa, and 50-hPa geopotential height (Figures 9b, 9c and 9d) all increased abruptly in 1978. The mean values of the periods after 1978 increased 14.2, 23 and 61.4 gpm than that of the forward periods, respectively. Figure 9c also notes that the DDAC occurred in 1993, and the average after 1993 is close to that in 1948–1977.

3.4. Autumn Averaged Fields

[24] Figures 10a, 10b and 10c show similar distributions of the DACs of SST, ULWRF and SAT which their DACs mainly occurred in 1975. The IDACs of SLP (Figure 10d) and 850-hPa geopotential height (Figure 10e) happened over the tropics in Eastern Hemisphere in 1975–1976, so did the IDACs of 500-hPa (Figure 10f) and 200-hPa geopotential height over the tropics in 1975–1976. The DDACs of SLP, 850-hPa and 500-hPa geopotential height took place over the Antarctica and circumpolar areas in 1974–1976. The 50-hPa IDACs (Figure 10h) occurred over the southern South Pacific in 1974, 1976–1977 and over the tropics and subtropics in 1978 except the equatorial domain.

[25] Figure 11a indicates that the IDACs of tropical geopotential height took place at 1000–150 hPa in 1976 and at 100–10 hPa in 1978 except the 20-hPa DACs in 1979. The IDACs of the South Indian Ocean (Figure 11b) happened at 700–20 hPa in 1974. The IDACs of the South Atlantic (Figure 11c) occurred at 925–200 hPa in 1974 and at 150–10 hPa in 1978.

[26] The IDACs of the southern tropical eastern Pacific SST (Figure 12a) occurred in 1975, with an enhancement 0.52°C of mean value. Figures 12b, 12c and 12d demonstrates the DACYs of the time series averaged from tropical geopotential height in 1976, 1976, and 1978, respectively. The mean values of the periods after each DACY increased 14.2, 23 and 61.4 gpm than that of the forward periods, respectively.

3.5. Winter Averaged Fields

[27] The distributions of the DACs of SST (Figure 13a), ULWRF (Figure 13b), SAT (Figure 13c), SLP (Figure 13d), and 850-hPa (Figure 13e), 500-hPa (Figure 13f) and 200-hPa geopotential height (Figure 13g) are similar to autumn ones, except the DDACs over the North Pacific in 1973 and 1975. Figure 13h exhibits that the IDACs happened over the latitudinal zone 45–90°S in 1973, over the Drake Passage in 1974, over the latitudinal zone 45°S–25°N in 1976 and over the northern subtropics in 1977–1978.

[28] Figure 14a shows that the IDACs of tropical geopotential height happened at 500–200 hPa in 1975 and at the other levels in 1976. The IDACs of the northern North Pacific (Figure 14b) took place at 1000–400 hPa in 1973. The IDACs of the central North Pacific (Figure 14c) occurred at 1000–250 hPa in 1975 and at 30–10 hPa in 1977. We remark here that the existence of IDACs at higher levels (Figure 14c) does not imply the region of IDACs had been propagated from low to high atmospheric levels in 3 a. As we presented above, the DAC scopes at high levels is much larger than that at low levels. Such situation may result from two independent processes.

[29] The IDACs of the southern tropical eastern Pacific SST (Figure 15a) occurred in 1975, with an enhancement 0.48°C of mean value. The DACYs of the time series of 500-hPa, 200-hPa and 50-hPa tropical geopotential height (Figures 15b, 15c and 15d) are 1975, 1975 and 1976 and the latter averages of these time series are 15.7, 23.8 and 58.4 gpm higher than the proceeding ones, respectively.

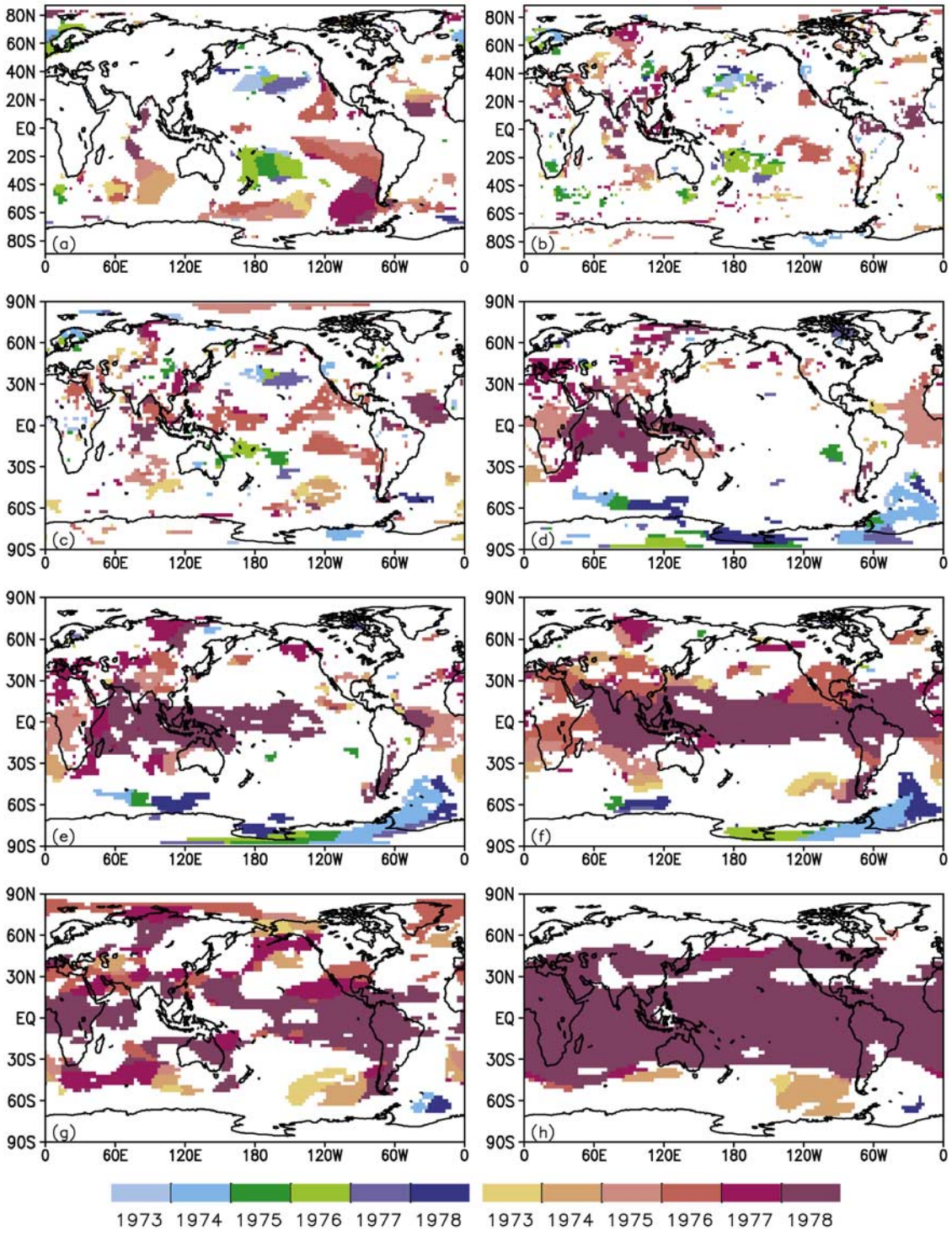

Figure 7. Same as Figure 1 but in summer averaged field.

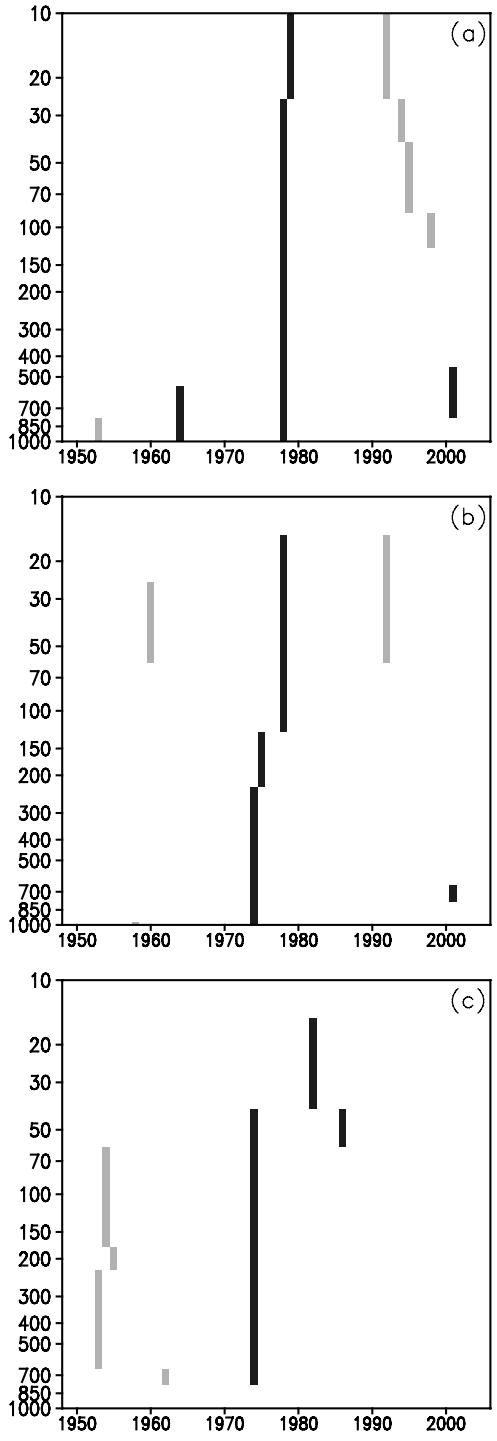

Figure 8. Same as Figure 2 but in summer averaged field in the regions (a) (20°S–20°N, 0°–357.5°E), (b) (30°–45°S, 10°W–20°E) and (c) (35°–50°S, 90°–120°E).

3.6. Seasonal Diversities

[30] We described the characteristics of the DACs in the 1970s of different seasons above. However, there are a few diversities of the DACYs in different seasons. The distributions of the DACYs in four seasons are similar generally. Therefore we only depict the seasonal diversities in a temporal sequence. The diversities of four seasons mainly existed in the tropics. The initial tropical oceanic DACs occurred in the tropical eastern Pacific in the summer of 1975 (Table 1). The original DACs of tropical atmosphere occurred over the tropical Atlantic and Middle Africa in the SLP and 850-hPa geopotential height fields at the same time. Such situations also existed in the autumn and winter of 1975. The DACs of several regions also extended to higher levels at the same time. The DACs of tropical eastern Pacific SST happened in the spring of 1976, so did the DACs over the tropical troposphere. In the sequent summer, the DACs of tropical eastern Pacific SST happened, so did that of Middle Africa of 500-hPa geopotential height. Sequentially, the DACs of several tropical tropospheric regions occurred in the autumn and winter of 1976. Afterward, the stratospheric DACs occurred in the spring of 1977, so did the SST and SAT DACs along the West American. Then, the tropospheric and stratospheric DACs occurred in the summer of 1978. The simultaneous DACs over the tropical Indian Ocean and tropical Atlantic happened in SST, SAT and ULWRF fields. The DACs of tropical Atlantic SST were concurrent with the DACs of stratospheric geopotential height in the autumn of 1978. It can be seen that the tropical SST DACs and the atmospheric ones were simultaneous in a certain period. Moreover, the atmospheric DACs over the North Pacific only occurred in the winter. The SH polar DACs happened in the winter of 1973.

4. Discussion

[31] In this section, we will draw upon the results presented above to address several questions designed to

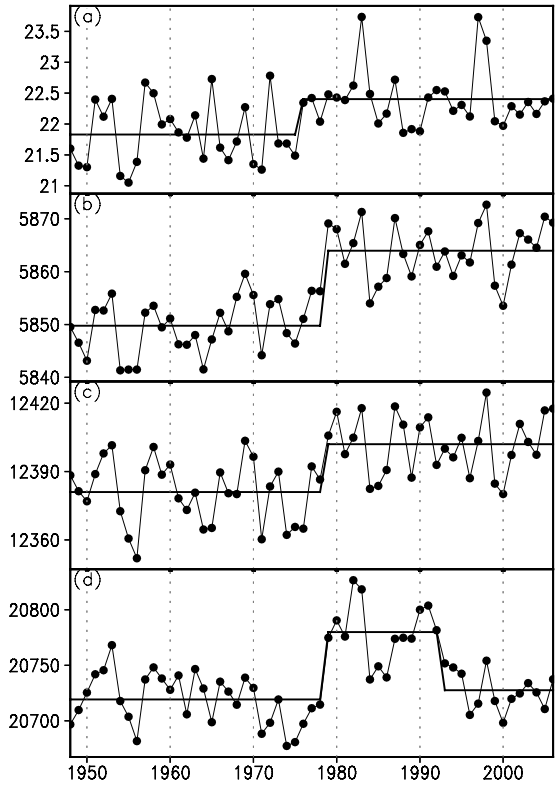

Figure 9. Same as Figure 3 but in summer averaged field in the areas (a) (8°–20°S, 120°–70°W), (b) (15°S–20°N, 0°–357.5°E), (c) (30°S–30°N, 0°–357.5°E) and (d) (35°S–35°N, 0°–357.5°E).

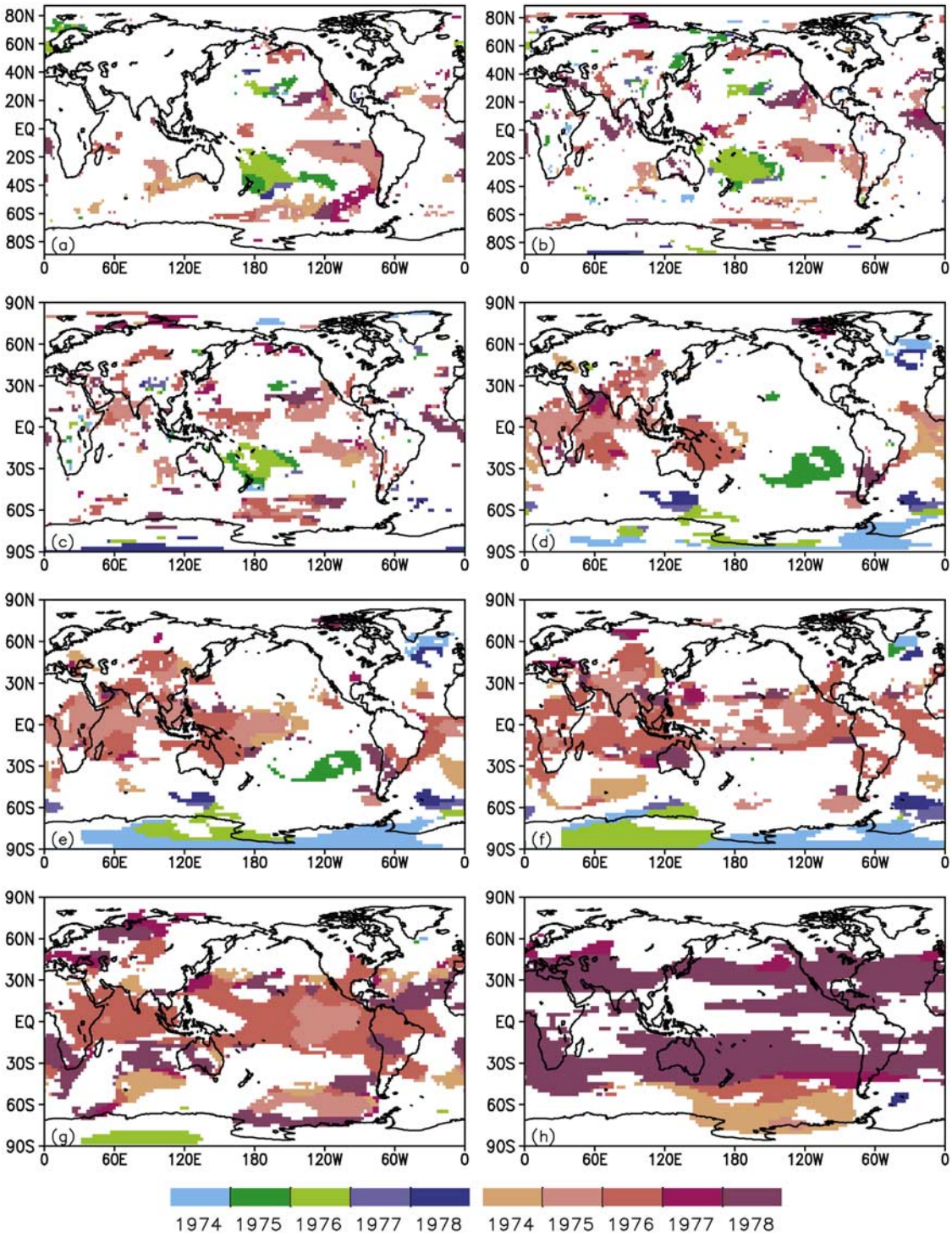

Figure 10. As in Figure 1 but in autumn averaged field.

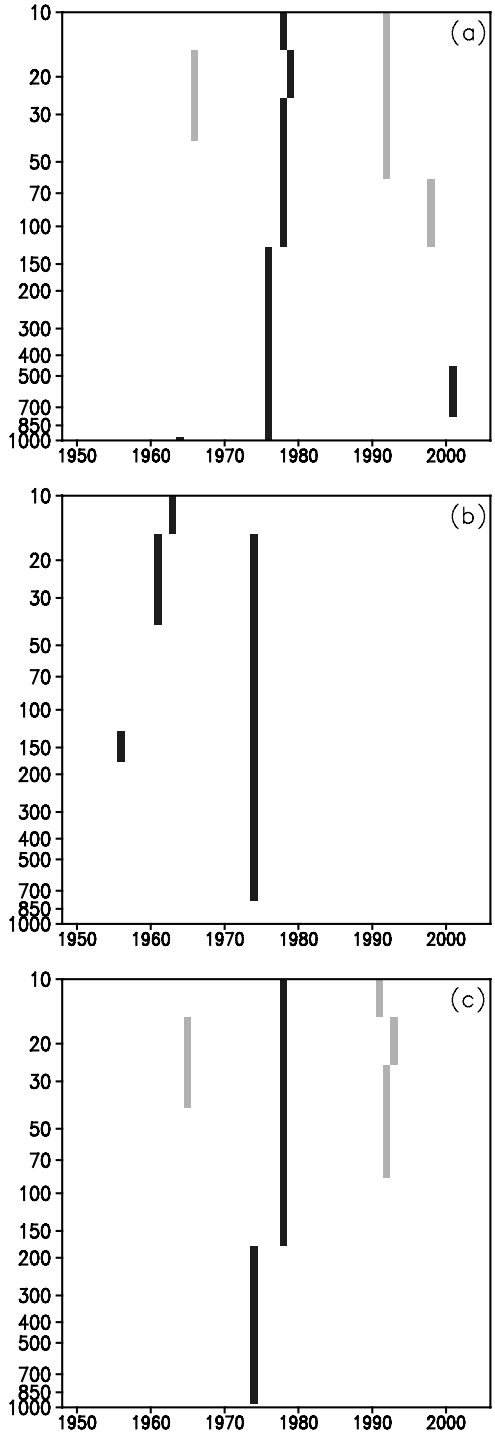

Figure 11. Same as Figure 2 but in autumn averaged field in the domains (a) (30°S–30°N, 0°–357.5°E), (b) (40°–55°S, 60°–120°E) and (c) (25°–45°S, 20°W–5°E).

explore the temporal relationships between the SST and atmospheric DACs in the 1970s.

[32] What are the temporal connections between the SST DACs of different oceanic regions in the 1970s? The oceanic DACs in the 1970s were global (Figures 1a, 4a, 7a, 10a and 13a). It can be seen in Table 2 that the initial SST DAC was in South Atlantic in the spring of 1973, followed with the North Pacific, South Pacific and South Indian Ocean in summer of 1973, and tropical Pacific in summer of 1975, etc. Thereby, the original DACs of the South Atlantic cannot be interpreted by that of tropical SST, which occurred about 2 a later than that of the South Atlantic, nor can the original SST DACs of North Pacific, South Pacific and South Indian Ocean, etc. The other oceanic DACs, except that of the North Pacific, cannot be attributed to the DACs over the North Pacific, which were not the initial oceanic DACs in the 1970s. Because several remote regions happened synchronously, it may be unsuitable to say that the DACs of the South Atlantic, which was the initial DAC regions in the 1970s, could interpret the rest oceanic DACs. Such global DACs may relate to the oceanic internal dynamic processes. The earlier DAC regions in this DACE, such as the South Atlantic, South Indian Ocean and the North and South Pacific, which may be the indicators of the global DACs, need to be further studied.

[33] What is the temporal relationship between the SST DACs and the atmospheric ones in the 1970s? The wind stress is an important atmospheric driving power of the surface oceanic flows. The DACs happened only in the winter of the zonal wind stress, not in other seasons and meridional wind stress field (in Figure 16a, others not shown). The IDACs occurred over the North Pacific in the winter of 1975, with a 25.6 N m^{-2} enhancement of mean value (Figure 16b). It means that the atmosphere over the North Pacific gave an enhanced forcing to the ocean

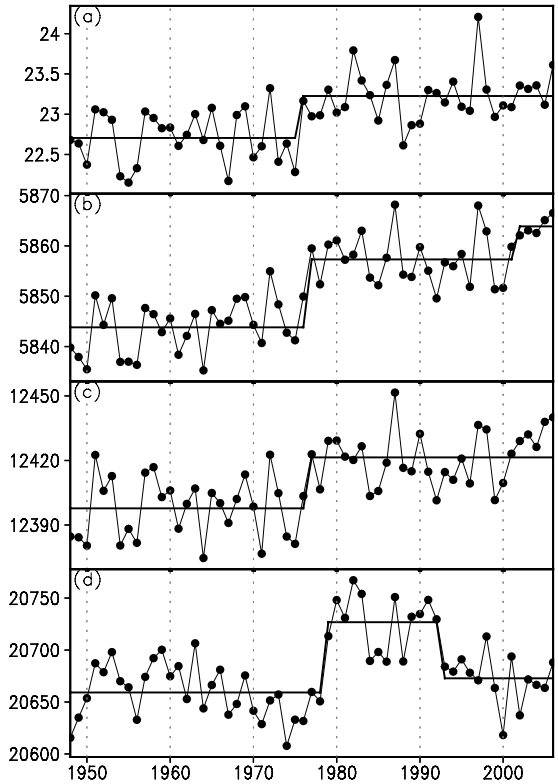

Figure 12. Same as Figure 3 but in autumn averaged field in the areas (a) (8–24°S, 150°–70°W), (b) (20°S–20°N, 0°–357.5°E), (c) (20°S–20°N, 0°–357.5°E) and (d) (40°S–40°N, 0°–357.5°E).

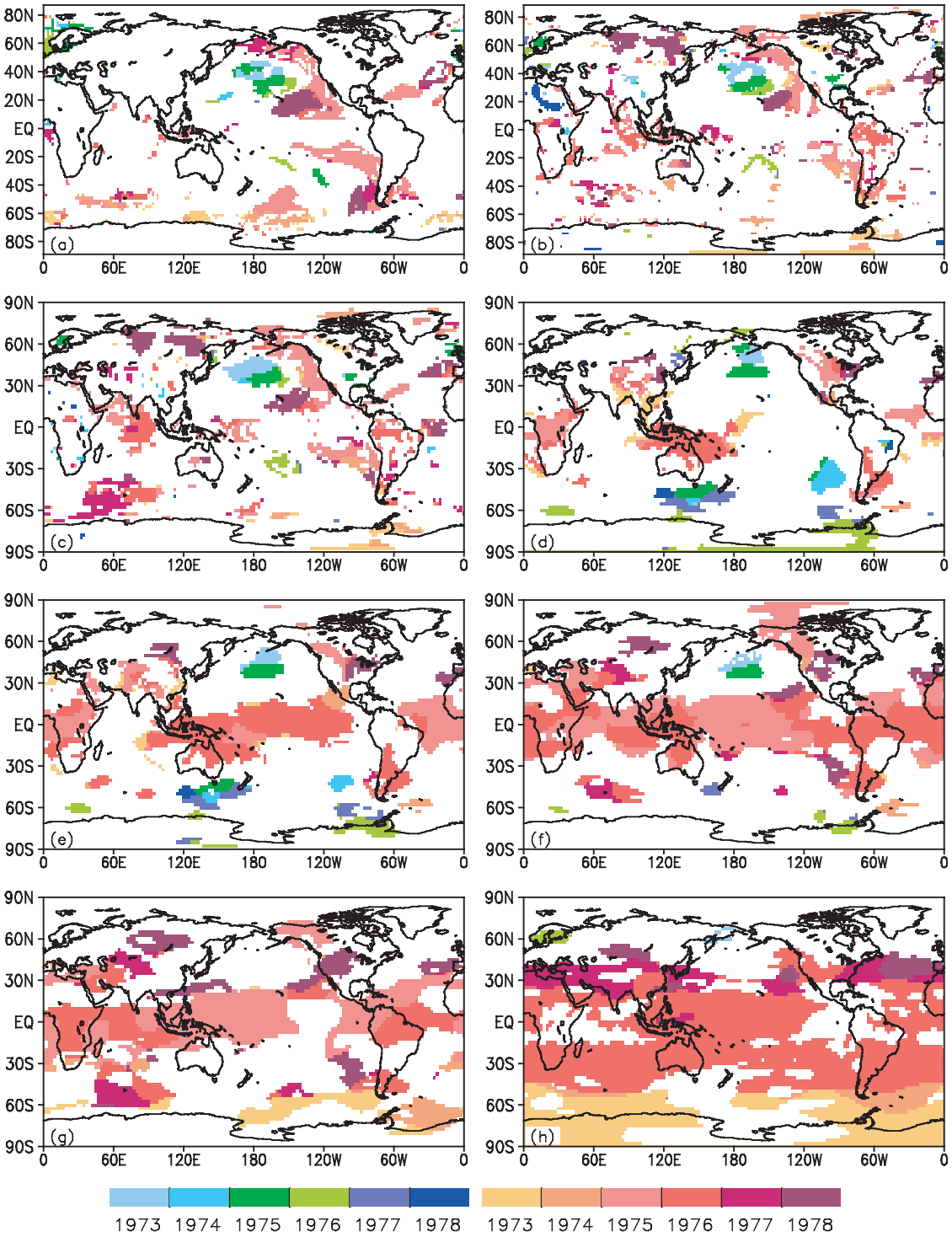

Figure 13. As in Figure 1 but in winter averaged field.

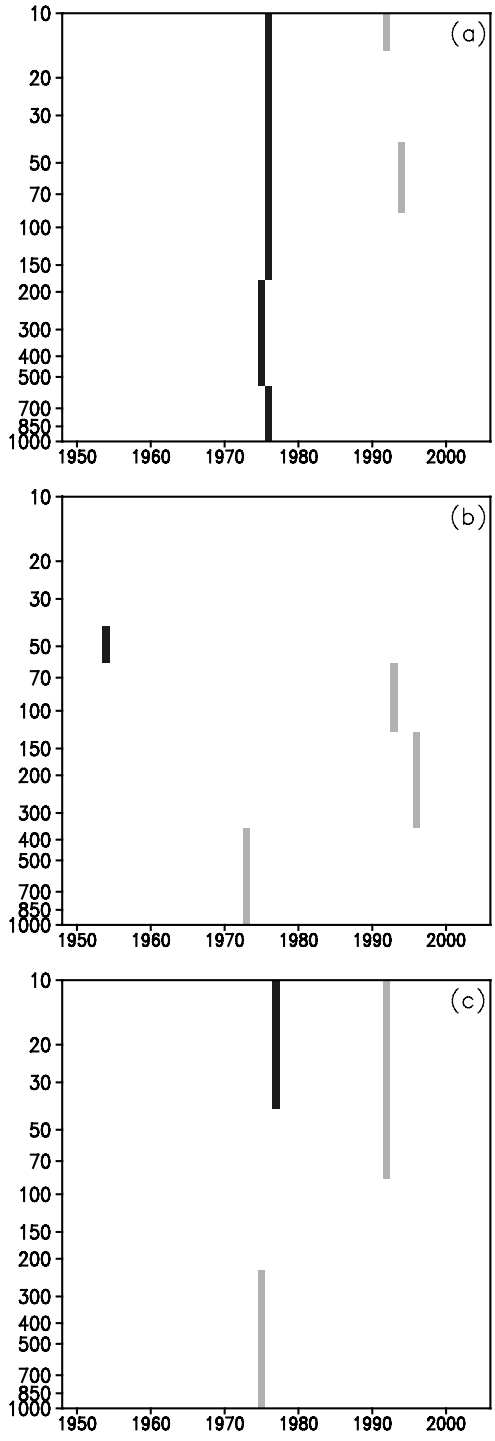

Figure 14. Same as Figure 2 but in winter averaged field in the regions (a) (20°S–20°N, 0°–357.5°E), (b) (45°–57.5°N, 170°E–150°W), and (c) (35°–42.5°N, 170°E–150°W).

since the winter of 1975. The initial DACs of global ocean and North Pacific occurred in the spring and summer of 1973 (Figures 4a and 7a), respectively. The initial oceanic DACs in the 1970s cannot be explained by that of the wind stress, which occurred about 2 a later than the initial oceanic DACs, nor can the initial SST DACs of the North pacific.

[34] What is the temporal connection between the extratropical SST DACs and extratropical atmospheric ones in this DACE? Table 3 shows the DACs exist in the extratropical SST and above atmosphere of several regions at several selected levels. The boldface and italics mean that there are no DACs in SST and lower troposphere, respectively. These DACs all happened in SH middle and high latitude. It may attribute to the relatively bad reliability of the SST and atmospheric data there or statistical methods. However, there are SST DACs and atmospheric ones in the other regions (white belts), without discontinuity. Moreover, within the hemispheric extent, it is showed in Table 1 that the initial NH extratropical SST DACs was earlier than the atmospheric ones and the initial SH extratropical atmospheric and SST DACs occurred synchronously in the spring of 1973. It seems that the extratropical SST DACs are generally simultaneous with the above atmospheric ones.

[35] We noted in preceding discussion that the DACs of winter zonal wind stress occurred about 2 a later than the initial DACs of North Pacific. However, in the winter, the DACs of zonal wind stress and SST of the North Pacific happened at the same year (Figures 16b and 16c). In addition, it is obvious to see the North Pacific influences on the atmospheric DACs of ULWRF, SAT SLP, geopotential heights (in Figure 13). These facts and possible reinforcement discussed below, both show the wintertime ocean-atmosphere decadal interaction over the North Pacific.

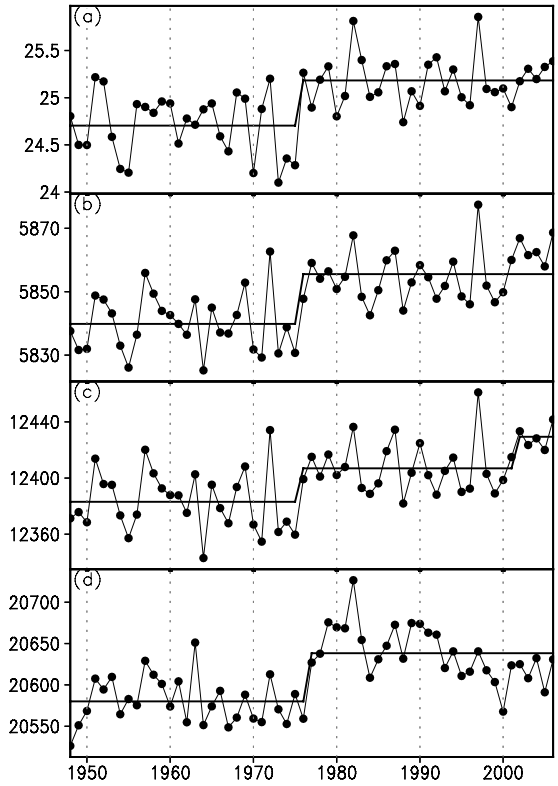

Figure 15. Same as Figure 3 but in winter averaged field in the areas (a) (8–24°S, 150°–70°W), (b) (20°S–20°N, 0°–357.5°E), (c) (30°S–20°N, 0°–357.5°E) and (d) (45°S–30°N, 0°–357.5°E).

Table 1. Occurrence Time and Locations of the Initial DAC in the 1970s of Several Variables, Including SST, SLP, and 850-hPa, 500-hPa, 200-hPa, and 50-hPa Geopotential Height (ght), in NH Extratropics, Tropics and SH Extratropics[a]

Variables	Occurrence Time and Locations in NH Extratropics	Occurrence Time and Locations in Tropics	Occurrence Time and Locations in SH Extratropics
SST	*JJA, 1973 (24°–34°N, 160°E–174°W)*	*JJA, 1975 (8°–20°S, 120°–70°W)*	*MAM, 1973 (34°–60°S, 50°–10°W)*
SLP	DJF, 1973 (45°–57.5°N, 170°E–150°W)	*JJA, 1975 (15°S–15°N, 50°W–40°E)*	*MAM, 1973, S*
850-hPa ght	DJF, 1973 (45°–57.5°N, 170°E–150°W)	*JJA, 1975 (20°S–10°N, 40°W–30°E)*	*MAM, 1973, S*
500-hPa ght	DJF, 1973 (45°–57.5°N, 170°E–150°W)	SON, 1975 (20°S–20°N, 160°E–120°W)	*MAM, 1973, S*
200-hPa ght	DJF, 1974 (52.5°–67.5°N, 35°–5°W)	SON, 1975 (15°S–15°N, 150°–90°W)	*MAM, 1973 (45°–55°S, 80°–30°W)*
50-hPa ght	DJF, 1977 (25°–35°N, 0°–357.5°E)	DJF, 1976 (45°S–30°N, 0°–357.5°E)	*MAM, 1973 (50°–60°S, 70°–40°W)*

[a]Italics indicate the initial DAC regions of above variables in NH extratropics, tropics and SH extratropics, respectively. "S" means that the DACs area is very small.

The westerly wind stress applied to the ocean surface in the NH causes the southward net mass transport within the Ekman layer. Significant temperature advection by this transport and the consequent cooling should be confined within the frontal region [*Frankignoul and Reynolds*, 1983]. The stronger the westerlies are, so are the transport and cooling, which acts to reinforce the negative SST anomalies there. The vertical structure of the winter atmospheric DACs over the North Pacific seems (Figures 14b and 14c) to support some GCM experiments [*Lau*, 1997] that propose a possible feedback from the midlatitude SST anomalies to the preexisting atmospheric anomalies aloft that have initially generated the SST anomalies. A feedback loop in our hypothesis may be closed. It is in agreement with the findings as suggested in coupled ocean-atmosphere GCMs [*Latif and Barnett*, 1994, 1996] and diagnostic analyses [*Nakamura et al.*, 1997]. Moreover, the IDACs of winter SST also occurred in 1986 and 1997. However, the DACs of winter zonal wind stress do not exist in the same region. Without the decadal anomalies of winter zonal wind stress, what are the causes and mechanisms of the DACs over the North Pacific? It is still an open question.

[36] What is the temporal relationship between the tropical SST DACs and the tropical atmospheric ones in the 1970s? It is known that the variation of atmosphere circulation is a quick process, so the tropical atmospheric DACs may result from the simultaneous forcing. That is, the atmospheric DACs may be a consequence by the forcing of one or more of them. Table 4 shows the SST DAC regions, which happened at the same time with the tropical atmospheric DACs. The tropical DAC domains of SST field mainly located in tropical Indian Ocean, tropical Atlantic and tropical eastern Pacific. Table 4 indicates that the Autumn DACs of tropical atmosphere are only accompanied by that of tropical SST. Moreover, the distribution of the ULWRF DACs was similar to that of the SST DACs, implying the possible places of SST forcing. Furthermore, Table 1 shows that the initial tropical DACs happened in SST, SLP and 850-hPa geopotential height field in the summer of 1973 and the initial higher-level tropical DACs occurred later than them. In addition, the tropical SST DACs and the tropical atmospheric DACs are concurrent in a certain period (shown above). These facts attach more importance to the decadal relationship between the tropical SST and atmosphere.

[37] If the tropical SST DACs and tropical atmospheric DACs are concurrent in the same locations in the 1970s (Table 4), then the open question is how were the decadal signals propagated to the whole tropical atmosphere? It is known that the Walker circulation weakened after late 1970s [*Nitta and Yamada*, 1989; *Kachi and Nitta*, 1997]. *Quan et al.* [2004] noted that the Hadley cell has been strengthening since 1950s. Further studies are needed to understand the roles of the Walker circulation and Hadley cell in the atmospheric DACs in the 1970s, in particular, the DACs associated with the global atmosphere-ocean system needs a long way to go.

[38] The most relevant temporal inhomogeneity in the assimilated data is probably the introduction of satellite observations which have dramatically improved the quality of the reanalyses over the last three decades [*Sturaro*, 2003]. Several study has emphasized the impacts of the temporal inhomogeneity in the assimilated data [e.g., *Bengtsson et al.*, 2004a, 2004b; *Dell'Aquila et al.*, 2005; *Sterl*, 2004]. Such temporal inhomogeneity in the assimilated data brings much doubt about the signals of the decadal variability in reanalysis data, which occurred in the same period of the introduction of unconventional observations, especially satellite data. It is necessary to discuss about the impacts of the introduction of satellite observations on the DACs of atmosphere-ocean system in the 1970s. The introduction of satellite observations since 1982 of ERSST.v2 [*Smith and Reynolds*, 2004] may not directly influence the reliability of the DACs of SST in the 1970s in this study. There are mainly two sources of satellite data for NCEP/NCAR reanalysis in the 1970s presented in detail by *Dell'Aquila et al.* [2005]. The first source of satellite data for reanalysis is the vertical temperature profile radiometer (VTPR), available from 1973 to 1978. If the VTPR data are temporal inhomogeneous with the observation data in the NCEP/NCAR reanalysis, there must be a sudden increase/decrease

Table 2. Occurrence Time and Locations of the Initial DACs in the 1970s of SST in Several Oceanic Basins

Locations of the Initial SST DACs in Several Oceanic Basins	Occurrence Time of the Initial SST DACs
North Pacific (24°–34°N, 160°E–174°W)	JJA, 1973
Tropical Pacific (8°–20°S, 120°–70°W)	JJA, 1975
South Pacific (46°–60°S, 150°–130°W)	JJA, 1973
Tropical Indian Ocean (20°S–18°N, 70°–90°E)	JJA, 1978
South Indian Ocean (40°–48°S, 50°–66°E)	JJA, 1973
North Atlantic (60°–70°N, 10°W–20°E)	MAM, 1974
Tropical Atlantic (20°–30°N, 70°–50°W)	DJF, 1975
South Atlantic (34°–60°S, 50°–10°W)	MAM, 1973

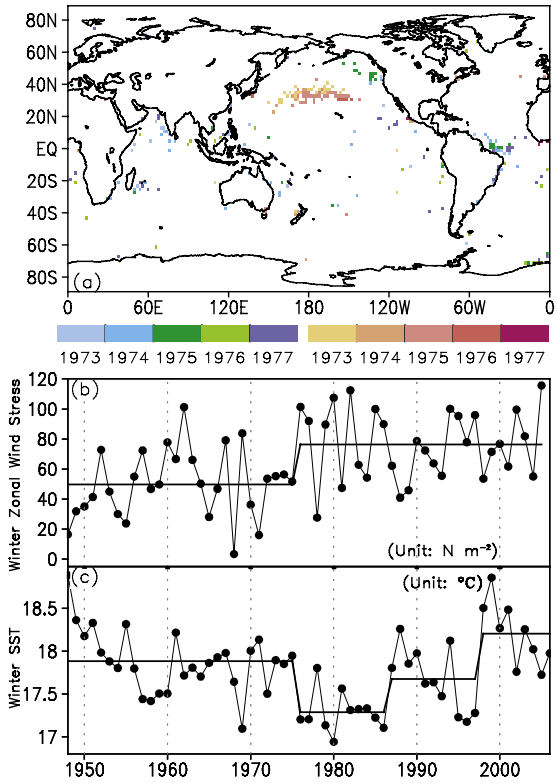

Figure 16. (a) Distribution of the DACYs of the winter zonal wind stress and the time series (solid circles) and episode averages (thickened solid line) of (b) winter zonal wind stress and (c) winter SST in the same domains (28°–38°N, 150°E–150°W). The DACYs, including Figures 16a, 16b and 16c, all exceed the 0.05 significant level. The false discovery rate of the DACYs of winter zonal wind stress is controlled at 0.05.

since 1973. Using the moving *t* test technique, the DACs wound have occurred in 1972. However, there were no DACs of atmosphere-ocean system in 1972 in this study. That is, there are no obvious influences on the DACs of atmosphere-ocean system in 1973–1978 after the VTPR data was introduced into NCEP/NCAR reanalysis. In addition, since 1979, the television infrared radiometer observation satellite (TIROS) operational vertical sounder (TOVS) data are available. The NCEP assimilates retrieved profiles of temperature and humidity. The authenticity of the atmospheric DACs in 1978 may be doubtable because of the similar hypothesis in the above case. The tropospheric and stratospheric DACs of geopotential height occurred in winter of 1975–1976, namely, the tropospheric and stratospheric geopotential height has increased since 1976–1977, prior to the introduction time of the TOVS data. At least, the atmospheric DACs which occurred before 1978 are creditable. As presented in section 3.6, the DACs of tropical SST in some regions may be concurrent with the tropical atmospheric DACs of certain regions from the summer of 1975 to the autumn of 1978. Moreover, the difference in NH between NCEP/NCAR and European Centre for Medium-Range Weather Forecasts (ECMWF) reanalyses is not found in monthly mean field in the analysis of *Sterl* [2004]. We tend to consider that the atmospheric DACs in 1978 may not attribute to the introduction of the TOVS data, which may be just coincident with the introduction time of the TOVS data.

5. Summary and Conclusion

[39] The horizontal, vertical and temporal characteristics of the DACs of atmosphere-ocean system in the 1970s are documented in our study. The DACs did not only occur in the winter of 1976, but also in all the seasons of the epoch 1973–1978. The DACs in the 1970s existed widely in the oceanic and atmospheric systems. In the ocean, the DDACs took place in the North and South Pacific and the IDACs mainly occurred in the eastern Pacific, southern South Pacific and South Indian Ocean. In the atmosphere, the IDACs happened over the Eastern Hemispheric tropics and subtropics in the low troposphere and over the global tropics and subtropics in the middle and upper troposphere and whole stratosphere. The higher pressure levels, the

Table 3. Occurrence Time, Locations, and Occurrence or Not of the Extratropical DACs in the 1970s of Several Variables, Including SST, and 850-hPa, 500-hPa, 200-hPa, and 50-hPa Geopotential Heights[a]

Occurrence Times and Locations of the Extratropical DACs	Variables				
	SST	850 hPa ght	500 hPa ght	200 hPa ght	50 hPa ght
1973, (40°–60°N, 170°E–150°W)	Y	Y	Y	N	N
1974, (35°–55°S, 80°–110°E)	Y	Y	Y	Y	Y
1974, (20°–40°S, 20°W–15°E)	Y	Y	Y	Y	N
1974, (45°–65°S, 135°–100°W)	*Y*	*N*	*Y*	*Y*	*Y*
MAM, 1973, (40°–50°S, 25°–50°E)	**N**	**Y**	**Y**	**Y**	**N**
MAM, 1973, (35°–50°S, 160°E–165°W)	**N**	**Y**	**Y**	**Y**	**N**
MAM, 1973, (50°–60°S, 75°–40°W)	Y	Y	Y	Y	Y
MAM, 1974, (25°–50°S, 80°–110°E)	Y	Y	Y	Y	N
JJA, 1973, (50°–60°S, 150°–130°W)	*Y*	*N*	*Y*	*Y*	*Y*
JJA, 1974, (30°–45°S, 10°W–20°E)	**N**	**Y**	**Y**	**Y**	**N**
JJA, 1974, (35°–50°S, 90°–120°E)	*Y*	*N*	*Y*	*Y*	*Y*
SON, 1974, (40°–55°S, 60°–120°E)	Y	Y	Y	Y	N
SON, 1974, (25°–45°S, 20°W–5°E)	Y	Y	Y	Y	N
SON, 1974, (45°–65°S, 160°–120°W)	*Y*	*N*	*N*	*Y*	*Y*
DJF, 1973, (45°–57.5°N, 170°E–150°W)	Y	Y	Y	N	N
DJF, 1975, (35°–42.5°N, 170°E–150°W)	Y	Y	Y	N	N

[a]"Y" means that there were DACs in the regions, and "N" represents contrariwise. Boldface and italics mean that there were no DACs in SST and lower tropospheric geopotential heights, respectively. Normal text represents that there were the DACs of SST and lower tropospheric geopotential heights of these regions, without discontinuity.

Table 4. Locations of the SST DACs Which Occurred at the Same Time With the DACs in the 1970s of the Tropical Geopotential Heights (Including 850-hPa, 500-hPa, 200-hPa, and 50-hPa Geopotential Heights)[a]

DACYs of Tropical Geopotential Height: Spring		
1976	1977	1978
(14°–24°S, 120°–70°W)	*(4°–20°N, 150°–110°W)*	*(4°–14°S, 124°–100°W)*
(30°–42°N, 150°E–160°W)	*(18°S–18°N, 110°–130°E)*	(36°–50°S, 100°–72°W)
	(24°–38°N, 175°–140°W)	
	(50°–64°S, 118°–76°W)	
	(50°–60°N, 178°E–140°W)	
DACYs of Tropical Geopotential Height: Summer, Autumn, Winter, and Annual		
1975	1976	1978
	Summer	
(10°–20°S, 120°–70°W)	*(16°–30°S, 120°–70°W)*	*(20°S–20°N, 60°–90°E)*
(18°–36°S, 180°–160°W)	*(4°–30°N, 140°–110°W)*	*(8°–18°N, 50°–24°W)*
(22°–36°S, 80°–100°E)	*(14°–42°S, 180°–162°W)*	(34°–50°S, 100°–70°W)
(54°–64°S, 130°E–140°W)	(20°–36°S, 160°–142°W)	
	Autumn	
(6°–22°S, 150°–70°W)	–	*(0°–18°S, 20°W–10°E)*
(6°–16°N, 130°–100°W)		
	Winter	
(6°–22°S, 150°–70°W)	–	N
(6°–16°N, 130°–100°W)		
(26°–36°N, 180°–150°W)		
(30°–40°S, 140°–106°W)		
	Annual	
N	*(6°–30°S, 150°–70°W)*	*(6°S–14°N, 66°–124°E)*
	(6°–20°N, 130°–100°W)	*(16°–26°N, 140°–120°W)*
	(20°–26°S, 178°E –150°W)	(36°–50°S, 100°–72°W)
	(26°–36°N, 176°E –156°W)	

[a]Dash means no DACs in SST field. "N" refers to no DACs in tropical atmosphere. The italicized domains lie in the tropics. The others lie in the extratropics.

larger the DAC scopes and the later the DACYs generally. Moreover, the DACs of extratropical atmosphere-ocean system are in advance of that of tropics. The atmospheric DACs presented in this study are associated with the DACs of global ocean, in agreement with earlier studies [*Zhang et al.*, 1997; *Deser et al.*, 2004]. These results extend our knowledge of the horizontal, vertical and temporal characteristics of the DACs of atmosphere-ocean system in the 1970s, especially the horizontal and vertical structures of the tropics. These findings offer more reasonable SST forcing fields and atmospheric evaluated standards for the numerical simulations of the DACs of atmosphere-ocean system in the 1970s, and offer the elementary decadal background for the interannual variability of ocean-atmosphere system.

[40] The initial oceanic DACs in the 1970s cannot be interpreted by the DACs of wind stress, which happened about 2 a later than the initial oceanic DACs. Furthermore, the original DDACs of the North Pacific cannot be attributed to the tropical DACs via the ocean and atmosphere, which occurred about 2 a later than the initial DACs of the North Pacific, nor can the DACs over the South Atlantic, South Indian Ocean and South Pacific. The DACs of the rest oceanic regions cannot be explained by the DDACs of the North Pacific, which were not the initial oceanic DACs in the 1970s. These facts and possible relationships and reinforcements between SST and atmosphere, as discussed above, suggest that the DACs of atmosphere-ocean system in the 1970s might initially originate from the ocean and a coupled atmosphere-ocean decadal interaction mechanism existed in the wintertime North Pacific.

[41] **Acknowledgments.** We thank J. Wang, J. Feng, and Y. Zhao for reading the manuscript carefully and giving us valuable suggestions that led to improvement. We wish to thank two anonymous reviewers for helpful comments. This work was jointly supported by 973 program (2006CB400503) and National Nature Science Foundation of China (40528006).

References

Barnett, T. P., D. W. Pierce, M. Latif, D. Dommenget, and R. Saravanan (1999), Interdecadal interactions between the Tropics and midlatitudes in the Pacific basin, *Geophys. Res. Lett.*, *26*, 615–618.

Bengtsson, L., S. Hagemann, and K. I. Hodges (2004a), Can climate trends be calculated from reanalysis data?, *J. Geophys. Res.*, *109*, D11111, doi:10.1029/2004JD004536.

Bengtsson, L., K. I. Hodges, and S. Hagemann (2004b), Sensitivity of the ERA40 reanalysis to the observing system: determination of the global atmospheric circulation from reduced observations, *Tellus, Ser. A*, *56*, 456–474.

Benjamini, Y., and Y. Hochberg (1995), Controlling the false discovery rate: A practical and powerful approach to multiple testing, *J. R. Stat. Soc. B*, *57*(1), 289–300.

Chao, Y., M. Ghil, and J. C. McWilliams (2000), Pacific interdecadal variability in this century's sea surface temperatures, *Geophys. Res. Lett.*, *27*(15), 2261–2264.

Chavez, F. P., J. Ryan, S. E. Lluch-Cota, and N. C. Miguel (2003), From anchovies to sardines and back: Multidecadal change in the Pacific Ocean, *Science*, *299*, 217–221.

Chen, T. C., H. van Loon, K. D. Wu, and M. C. Yen (1992), Changes in the atmospheric circulation over the North Pacific–North America area since 1950, *J. Meteorol. Soc. Jpn.*, *70*, 1137–1146.

Chen, T. C., J. M. Chen, and C. K. Wikle (1996), Interdecadal variation in U.S. Pacific coast precipitation over the past four decades, *Bull. Am. Meteorol. Soc.*, *77*, 1197–1205.

Dell'Aquila, A., V. Lucarini, P. M. Ruti, and S. Calmanti (2005), Hayashi spectra of the northern hemisphere mid-latitude atmospheric variability in the NCEP-NCAR and ECMWF reanalyses, *Clim. Dyn.*, *25*, 639–652.

Deser, C., and M. L. Blackmon (1995), On the relationship between tropical and North Pacific sea surface temperature variations, *J. Clim.*, *8*, 1677–1680.

Deser, C., A. S. Phillips, and J. W. Hurrell (2004), Pacific interdecadal climate variability: linkages between the tropics and the North Pacific during boreal winter since 1900, *J. Clim.*, *17*, 3109–3124.

Dowton, M. W., and K. A. Miller (1993), The freeze risk to Florida citrus II: Temperature variability and circulation patterns, *J. Clim.*, *7*, 364–372.

Frankignoul, C., and R. W. Reynolds (1983), Testing a dynamical model for midlatitude sea surface temperature anomalies, *J. Phys. Oceanogr.*, *13*, 1131–1145.

Graham, N. E. (1994), Decadal-scale climate variability in the tropical and North Pacific during the 1970s and 1980s: Observations and model results, *Clim. Dyn.*, *10*, 135–162.

Graham, N. E., T. P. Barnett, R. Wilde, M. Ponater, and S. Schubert (1994), On the roles of tropical and midlatitude SSTs in forcing interannual to interdecadal variability in the winter Northern Hemisphere circulation, *J. Clim.*, *7*, 1416–1442.

Gu, D. F., and S. G. H. Philander (1997), Interdecadal climate fluctuations that depend on exchanges between the tropics and extratropics, *Science*, *275*, 805–807.

Huang, J. Y. (2000), *Statistic Analysis and Forecast Methods in Meteorology*, pp. 25–27, China Meteorol. Press, Beijing.

Jiang, J. M., and X. T. You (1996), Where and when did an abrupt climatic change occur in China during the last 43 years?, *Theor. Appl. Climatol.*, *55*, 33–40.

Jiang, J. M., K. Fraedrich, and Y. R. Zou (2001), A scanning t-test of multiscale abrupt changes and its coherence analysis, *Chin. J. Geophys.*, *44*(1), 31–39.

Kachi, M., and T. Nitta (1997), Decadal variations of the global atmosphere-ocean system, *J. Meteorol. Soc. Jpn.*, *75*, 657–675.

Kalnay, E. M., et al. (1996), The NCEP/NCAR reanalysis project, *Bull. Am. Meteorol. Soc.*, *77*, 437–471.

Latif, M., and T. P. Barnett (1994), Causes of decadal climate variability over the North Pacific and North America, *Science*, *266*, 634–637.

Latif, M., and T. P. Barnett (1996), Decadal climate variability over the North Pacific and North America: Dynamics and predictability, *J. Clim.*, *9*, 2407–2423.

Lau, N.-C. (1997), Interactions between global SST anomalies and the midlatitude atmospheric circulation, *Bull. Am. Meteorol. Soc.*, *78*, 21–33.

Li, Y., W. Cai, and E. P. Campbell (2005), Statistical modeling of extreme rainfall in southwest western Australia, *J. Clim.*, *18*, 852–863.

Mantua, N. J., S. R. Hare, Y. Zhang, J. M. Wallace, and R. C. Francis (1997), A Pacific interdecadal climate oscillation with impacts on salmon production, *Bull. Am. Meteorol. Soc.*, *78*, 1069–1079.

Minobe, S. (1997), A 50–70 year climatic oscillation over the North Pacific and North America, *Geophys. Res. Lett.*, *24*, 683–686.

Nakamura, H., G. Lin, and T. Yamagata (1997), Decadal climate variability in the North Pacific during the recent decades, *Bull. Am. Meteorol. Soc.*, *78*(10), 2215–2225.

Nitta, T., and S. Yamada (1989), Recent warming of tropical sea surface temperature and its relationship to the Northern Hemisphere circulation, *J. Meteorol. Soc. Jpn.*, *67*, 375–383.

Quan, X. W., H. F. Diaz, and M. P. Hoerling (2004), Change in the tropical Hadley cell since 1950, in *The Hadley Circulation: Past, Present, and Future*, edited by H. F. Diaz, and R. S. Bradley, pp. 85–120, Cambridge Univ. Press, New York.

Smith, T. M., and R. W. Reynolds (2004), Improved extended reconstruction of SST (1854–1997), *J. Clim.*, *17*, 2466–2477.

Sterl, A. (2004), On the (in)homogeneity of reanalysis products, *J. Clim.*, *17*, 3866–3873.

Sturaro, G. (2003), A closer look at the climatological discontinuities present in the NCEP/NCAR reanalysis temperature due to the introduction of satellite data, *Clim. Dyn.*, *21*, 309–316.

Trenberth, K. E. (1990), Recent observed interdecadal climate changes in the Northern Hemisphere, *Bull. Am. Meteorol. Soc.*, *71*, 988–993.

Trenberth, K. E., and J. W. Hurrell (1994), Decadal atmospheric-ocean variations in the Pacific, *Clim. Dyn.*, *9*, 303–319.

Vimont, D. J., D. S. Battisti, and A. C. Hirst (2001), Footprinting: A seasonal connection between the tropics and mid-latitudes, *Geophys. Res. Lett.*, *28*, 3923–3936.

Wang, B. (1995), Interdecadal changes in Niño onset in the last four decades, *J. Clim.*, *8*, 267–285.

Wu, L. X., and Z. Y. Liu (2003), Decadal variability in the North Pacific: The eastern North Pacific mode, *J. Clim.*, *16*, 3111–3131.

Zhang, Y., J. M. Wallace, and D. S. Battisti (1997), ENSO-like interdecadal variability: 1900–93, *J. Clim.*, *10*, 1004–1020.

J. Li and D. Xiao, National Key Laboratory of Atmospheric Sciences and Geophysical Fluid Dynamics, Institute of Atmospheric Physics, Chinese Academy of Sciences, Beijing 100029, China. (ljp@lasg.iap.ac.cn; xiaodong@mail.iap.ac.cn)